IMPLEMENTATION OF CLAHE CONTRAST ENHANCEMENT & OTSU THRESHOLDING INRETINAL IMAGE PROCESSING

T M SOUJANYA[1],K PRASAD BABU[2]

[1]DECS 202T1D3807, ASHOKA WOMENS ENGINEERING COLLEGE, KURNOOL, A.P.
[2]AssociateProfessor–ASHOKA WOMENS ENGINEERING COLLEGE, KURNOOL, A.P

ABSTRACT

In both ophthalmological and cardiovascular disease diagnosis, the accurate segmentation of the retinal vessel tree has become the prerequisite step for automatic or computer-aided diagnosis systems. Unlike typical foreground and background segmentation in normal image processing, there are three problems making the retinal vessel segmentation task even harder. First, the retinal color image tends to be red everywhere, thus having a lower contrast than normal image segmentation. Second, most retinal color images suffer from unbalanced illumination and make it harder to recognize background. Third, the symptom for retinopathy has unexpected color and shape, thus making it more difficult to separate vessel from noises. Under such circumstance, the research of the retinal blood vessel segmentation has brought much attention and been developed. In this work, the input is a retinal color image and the output will be a binary image of the vessel and non-vessel pixels. Preprocessing with CLAHE contrast enhancement, Vessel Extraction with Otsu thresholding is implemented along with performance parameters Accuracy, Sensitivity and Specificity. In the proposed work 20 images are used from the database called Digital Retinal Images for Vessel Extraction. Te performance parameters Specificity, Sensitivity, Accuracy are evaluated.

Key Words - Retinal image, Blood vessels segmentation, Accuracy, Sensitivity and Specificity

1. Introduction

The retinal blood vessel has been acknowledged as an indispensable element in both ophthalmological and cardiovascular disease diagnosis such as glaucoma and diabetic retinopathy. The attributes of retinal vasculature including length, width, tortuosity, branching pattern and angles will contribute to the diagnostic result. However, manual segmentation of retinal blood vessels, although possible, is a time consuming and repetitive work, and it also requires professional skills for even the thinnest vessel could contribute to the differential diagnosis list. In order to assist ophthalmologists with this complex and tedious work, the demand for the fast automated analysis of the retinal vessel images arises. Since the study of retinal blood vessel segmentation was firstly published in 1989, almost 30 years have passed, magnificent improvement has been made to this study with the development of public retinal image databases, advanced image processing algorithms, and supervised machine learning techniques. To understand how those developments has effectively contributed to the performance of retinal vessel segmentation.Retina is the photo sensitive, innermost tissue layer of the eye. It is located near the optic nerve. The Retina's function is to receive light that our eye lens has focused, convert it into neural signals, and send the signals on to the brain for visual recognition. The central retinal artery and vein, and their branches are the retinal blood vessels. It is thus an extension of the brain . The diseases of the eye, as well as diseases that affect the circulation and the brain can manifest themselves in the retina because of the architecture. The retina is vulnerable to organ specific and systemic diseases, imaging the retina allows diseases of the eye proper, as well as complications of diabetes, hypertension, and other cardiovascular diseases, to be detected, diagnosed, and managed. The deep- rooted blood vessel of the eye is only observed in a non-invasive manner. The fundus photography and optical coherence tomography image analysis is used to provide comprehensive descriptions of retinal morphology and function. The visible parts of the eye are the transparent cornea, the white sclera, the iris and an opening in the iris, the normally black pupil. A ray of light after passing through the cornea, which focusses the image partially, passes through the pupil, the lens which focuses the image further, the vitreous and is then focused on the retina. The retina is supported by the retinal pigment epithelium,

which is opaque. The primary blood supply to retina is through choroid and secondarily through retinal vasculature that lies on top of the retina. It is useful to divide the retina and choroid into the following layers:

1. internal limiting membrane.
2. nerve fiber layer (the axons of the ganglion cells, that transmit the visual signal to the lateral geniculate nucleus and thence the visual cortex).
3. ganglion cell layer (the cell bodies of the ganglion cells).
4. inner plexiform layer (the axons of the bipolar cells).
5. inner nuclear layer (the cell bodies of the bipolar and horizontal cells).
6. outer plexiform layer (the dendrites of the horizontal cells and the inner segments of the rod and cone photoreceptor cells).
7. outer nuclear layer (cell bodies—outer segments—of the photoreceptor cells)
8. external limiting membrane.
9. pigment epithelium.
10. Bruch's membrane.
11. capillary choroid (capillaries of the choroid)
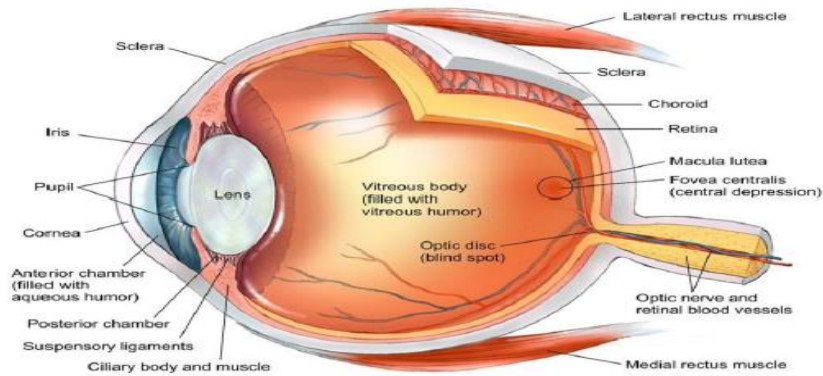12. choroid plexus.
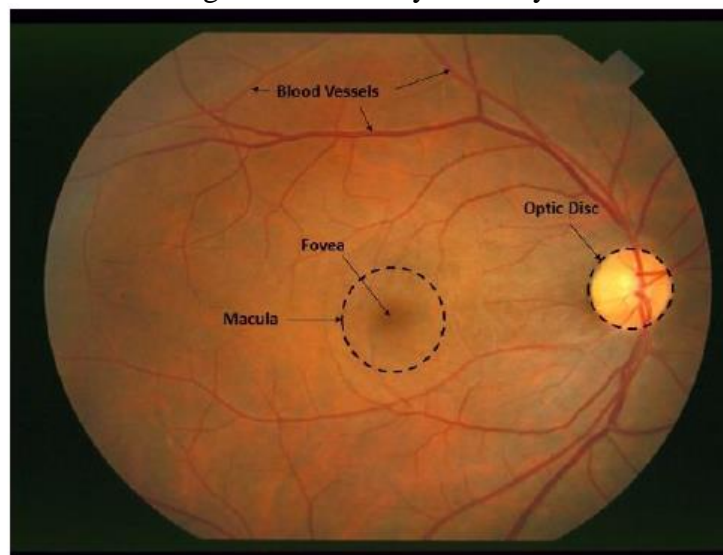

Figure 1 : Anatomy of the eye

Figure2 : Anatomy of the retina

The retina is a thin membrane that lies in the innermost surface of the eye. It is a thin layer of light-sensitive tissue that receives the light rays passed through the cornea and lens. Those lights are converted into electrical impulses by the retina and are sent to the brain via the optic nerve and then the brain expounds them as an image. The cornea and lens act like the camera lens, while the retina acts like the film. Therefore, the retina captures blurry images when the cornea and lens do not

focus the images properly. The retina comprises two types of photoreceptors, rods and the cones, responsible for visual phototransduction

FUNDUS PHOTOGRAPHY

Fundus photography involves photographing the rear of an eye; also known as the fundus. Specialized fundus cameras consisting of an intricate microscope attached to a flash enabled camera are used in fundus photography. The main structures that can be visualized on a fundus photo are the central and peripheral retina, optic disc, and macula. Fundus photography can be performed with colored filters, or with specialized dyes including fluorescein and indocyanine green. Practical instruments for fundus photography perform the following modes of examination:

• Color, where retina is illuminated by white light & examined in full color.

• Red free fundus photography utilizes a filter in order to better observe superficial lesions and some vascular abnormalities within the retina and surrounding tissue. A green filter 540–570 nm is used to block out red wavelengths of light. This allows a better contrast for viewing retinal blood vessels and associated hemorrhages, pale lesions such as drusen and exudates, and subtle characteristics such as nerve fiber layer defects and epiretinal membranes. This is a method of better observing intraretinal microvascular abnormalities, neovascularization at the disc and elsewhere in Diabetic retinopathy progression assessment. Red free photography is also regularly used as a base line photo prior to Angiography.

• Angiography is a process of photographing vascular flow within the retina and surrounding tissue by injecting a fluorescent dye into the blood stream. This dye fluoresces a different color when light from a specific wavelength reaches it. Using this method, a sequence of photographs can be produced that show the movement, and pooling of blood over time as the dye passes through the retina and choroid.

• Sodium Fluorescein Angiography is used for the imaging of retinal vascular disease and utilizes blue excitation light of 490 nm and fluoresces a yellow light of 530 nm. It is routinely used to image Cystoid Macular Oedema and Diabetic Retinopathy, among others.

Retinal Image Screening Techniques

There is a wide range of cameras to capture the retinal image. For obtaining the retinal fundus images, the cameras are classified into mydriatic and non-mydriatic retinal image cameras. To capture the retina images using the mydriatic camera, it is required to dilate the retina by administrating dilatation drops into the eyes of the patient. This camera is used especially in those cases where the pupil of the patient is ≤ 4 mm. A non-mydriatic camera is the most commonly used tool for acquiring the retinal fundus images. Fig. 1.3 shows two very popular non-mydriatic cameras: (a) Canon CR6-45NM (Canon USA, Lake Success, EEUU) and (b) Topcon TRC-NW6S (Topcon America Corp., Paramus, EEUU). The ophthalmologists and optometrists can immediately capture ultra-high-resolution digital images of the retina using these cameras.

Figure 3: Two types of non-mydriatic retinal image cameras: (a) Canon CR6-45NM and (b) Topcon TRC-NW6S

RETINAL MANIFESTATIONS OF EYE AND SYSTEMIC DISEASE
The most prevalent diseases that can be studied through eye imaging and analysis are as follows.
A. Diabetic retinopathy: In early stages, high blood sugar damages the blood vessels in the retina, they can either leak fluid or bleed. This can cause the retina to swell and form deposits. In later stages, leakage from blood vessels into the eye's vitreous humor can cause severe vision problems and will eventually lead to blindness. Diabetic retinopathy can often be prevented with early detection, proper management of diabetes and routine eye examination performed by ophthalmologist.
B. Age-Related Macular Degeneration: Age Related Macular Degeneration affects the macula. A patient with macular degeneration gradually loses central vision but maintains peripheral or side vision. Blindness is rare in macular degeneration. The leading cause of vision loss among older Americans is Macular degeneration. According to statistics, one-third of males and one-quarter of females over 75 have some form of Age-related Macular Degeneration. The prevalence of macular degeneration and the severity of vision loss increases with age.
C. Hypertensive Retinopathy: Chronic high blood pressure can damage the tiny blood vessels that nourish the retina, leading to significant vision problems. Risk factors for hypertensive retinopathy are the same as those for high blood pressure, including obesity, lack of physical activity, eating too much salt, a family history of hypertension and a stressful lifestyle. Hypertension can invoke direct retinal ischemia, which causes retinal infarcts visible as cotton wool spots and choroidal infarcts visible as deep retinal white spots.
D. Macular edema: This is an accumulation of fluid and swelling of the macula, causing distortion, and blurred central vision. Macular edema has several causes, including diabetes. In some cases, swelling of the macula can occur after cataract surgery.
E. Cardiovascular disease: The A/V ratio, the ratio between the diameter of arteries and veins of the veins changes due to atherosclerosis and hypertension. A decrease in A/V ratio, that is, widening of veins and thinning of arteries, is associated with stroke and myocardial infarction.

2. Literature Survey

The literature on the detection of retinal blood vascular disease is mostly dominated by the research works for Diabetic Retinopathy (DR) detection. A few research groups have focused on the detection of other retinal blood vascular diseases. Various algorithms for Hypertensive Retinopathy detection, using blood vessels as features, are proposed by the researchers in (Ortíz et al. 2010; Agurto et al. 2014; Irshad et al. 2015; Khitran et al. 2015; Syahputra et al. 2017). The Central Retinal Artery Occlusion detection methodology is presented by (Foroozan, Savino &Sergott 2002; Riccardi, Siniscalchi&Lerza 2016). In this dissertation, the research is mostly concerned about two leading causes of blindness, viz., Diabetic Retinopathy and Retinal Vein Occlusion, therefore, the literature review provided here is limited to these two particular diseases only. The state-of-the-art for DR detection and RVO detection has been explored in two subsections. In each subsection, the existing methods have been discussed and summarized in tabular form.

State-of-the-Art of DR Detection
In the past ten years, several research works have been carried out in order to develop automated DR diagnosis methods using different clinical features such as microaneurysms, haemorrhages, exudates, blood vessels, node points, and textures, etc. Those methodologies are mainly dependent on the segmentation of bright lesions and red lesions, comprising several steps. By following the general rules of any CAD method, first, pre-processing is carried out to boost the quality of the image by normalizing the original retinal image (Spencer et al. 1996; Takahashi & Kajikawa 2017). Second, segmentation methods are performed to identify the anatomical components of the retina, such as the optic disk and blood vessels (Jelinek et al. 2007; Salamat, Missen& Rashid 2019). Finally, after removing the normal features of the retina, the residual features are extracted as the possible pathologies of DR for the particular classification task. In this section, an extensive survey has been provided on available algorithms for automatic retinal image analysis to detect DR features. Different methodologies have

been discussed individually as the algorithms for bright lesion segmentation, algorithms for red lesion segmentation, DR screening system, and deep learning methods; and are illustrated in the following subsections.

Segmentation of Bright Lesions:
The bright lesions found in DR are mainly Hard-Exudates and Cotton Wool Spots. These bright lesions are lipoprotein deposited in the retina due to vascular leakage (Ali et al. 2013; Scanlon 2019). As discussed in the Chapter-2, Section 2.5.2; these bright lesions appear as yellow-whitish lesions. The hard exudates have well-defined edges, whereas, the cotton wool spots have indistinct edges, thus also called soft-exudates. The size, shape, brightness, and location of these lesions may vary among different patients (Fleming et al. 2007; Scanlon 2019). The researchers have provided various methods for detection of exudates using morphological operation, region growing, wavelet-based, and neural network. These methods can be categorized into four groups (Giancardo et al. 2012; Amin, Sharif & Yasmin 2016)

1. Region Growing Methods
The region growing method of segmentation is the dividing an image into homogenous regions of connected pixels based on the similarity criteria of the candidate pixels. The similarity criteria mainly include the shared characteristics of the candidate pixels, such as intensity, color, and texture. These techniques involve initialization of a seed point from a particular pixel point. Then, the images are segmented based on the similar intensity values of the neighbouring pixels. The process iterates until all the homogenous pixels are included in a region starting from the seed point. A few researchers used this technique to segment exudates (Sinthanayothin et al. 2003; Lariche, Kalkhajeh&Lodariche 2017). Sinthanayothin et al. have proposed a thresholding based method to identify the homogeneous pixels in the exudates. Then, using recursive region growing technique the exudates were detected in as pixels with similar grey level (defined by the manually selected threshold) are considered as pixels belonging to the same exudate region (Sinthanayothin et al. 2003)

2. Thresholding Methods
These types of methods segment the suspicious region using the difference between the foreground and background intensity level. The adaptive gray level analysis is the most common method used by various researchers to detect exudates. Sánchez *et al*. proposed a color feature-based approach, where the intensity of various pixels is projected to a new color space by modifying the RGB model (Sánchez et al. 2006, 2008). Jaafar et al. have proposed an adaptive thresholding method, where the image has been divided into homogeneous regions and then, adaptive thresholding has been applied to each individual region (Jaafar, Nandi & Al-Nuaimy 2011b). Win et al. have used thresholding method to detect exudate by eliminating the optic disc considering the fact that the appearance of optic disc resembles the exudates (bright yellowish region). By cropping the optical disc manually, a template was created with the calculated histogram of the optic disc. With the help of histogram matching the optic disc region was removed from the retina image. Then, the retina image was divided into left and right part. In order to detect exudates, Otsu thresholding method has been used by feeding the histogram difference of the right and left half of the optic disc removed retina (Win &Choomchuay 2017). Long et al. used a combination of dynamic thresholding and global thresholding method based on Fuzzy C-means clustering to detect the candidate exudates. The retina image was divided into sub-images and then Fuzzy C-means clustering was used to get the local dynamic threshold in each sub-image. Each pixel was assigned to different category in a sub-image. In this way, entire retina image was classified to generate the global threshold matrix. This combination is used to obtain the final threshold to segment candidate exudates region in the color retinal images. To segment the exudates from the exudate region, six texture features are extracted, viz., mean green channel intensity, gray intensity, energy, mean hue, mean gradient magnitude, and standard deviation. These features are fed to a support vector machine to classify the exudates and no exudate region (Long et al. 2019).

3. Mathematical Morphology Operations
Morphological operators are useful to detect structures with definite shapes. Here, each pixel value is adjusted relative to the values of the neighbouring pixels in order to construct a morphological operation

sensitive to specific shapes in an image, known as a structuring element. Based on the characteristics of the target shape the structuring elements are encoded and process the image with certain mathematical operations (e.g. erosion and dilation). Therefore, it is a popular method for the segmentation of different shapes. A two-scale segmentation method is proposed for exudates detection in (Sopharak et al. 2008; X. Zhang et al. 2014). A top-hat operator is applied to the green channel of the retinal image to identify small exudates. The large exudates are detected by filtering and thresholding method after performing a morphological restoration in (X. Zhang et al. 2014). Ghaffar et al. proposed a morphological tree for segmentation of exudates. Initially, blobbing technique is used to identify all the connected pixels as a single blob. The blobs with very large area are discarded by passing all the blobs through an area filter. The remaining blobs are further categorised into small, medium, and large. The medium blobs are pre-processed in order to remove the strong boundaries and get the candidate suspected regions/location. All the candidate blobs are passed through the morphological compact tree, which contains a series of filters with different criteria to remove the non-exudate regions. The filters those separate exudate and non-exudate regions are: area of the blob, mean, minimum and maximum hue of the blob, minimum and maximum intensity of the graycolor image and red and green color channels of the image, mean, maximum, and minimum saturation of the blob. The threshold of each of these filters is set manually for different images (Ghaffar et al. 2016).

4. Classification Methods:

These methods typically use machine learning approach to classify different patterns from the input features. Some of the popular classifiers are Support Vector Machine, Artificial Neural Network, Radial Basis Function, Decision Tree, k-Nearest Neighbouring, etc. With the help of various feature engineering processes as discussed above, the candidate features are fed to a classifier, then, the classifier learns the internal pattern to classify them into the target classes. In case of DR detection, various classifiers have been used to separate hard exudates from other kinds of bright lesions such as Cotton Wool Spots and drusen. In (Osareh, Shadgar& Markham 2009) candidate exudates are selected from the LUV color space and fuzzy c-means clustering is used as an efficient coarse to fine segmentation. Garcia et al. applied a similar approach for coarse segmentation of bright image regions, with a combined global and adaptive histogram thresholding method. After feature extraction, the performance is assessed by three classifiers: Multilayer perceptron, radial basis function, and support vector machine (García et al. 2010)

Fleming et al. have used a multi-scale morphological process for candidate exudates detection. The candidate regions are classified as exudates, drusen or background by an SVM (Fleming et al. 2007). Niemeijer et al. have proposed a clustering method where pixels are grouped into exudates and non-exudates through a lesion probability map generated by an assigned probability value for each pixel. Based on the cluster characteristics, each pixel has been classified as either exudates or non-exudates region and then, a k-NN classifier and a linear discriminant classifier is used to classify bright lesions into hard exudates, soft exudates, and drusen. (Niemeijer et al. 2007).

Ruba et al. have used Gabor features and GLCM features to extract the texture information of the exudates region. Gabor filter, which is used mainly as edge detection filter, has been used to extract 24 features including variance, mean, and standard deviation from the different orientation of the image. Then Grey Level Occurrence Matrix (GLCM) has been calculated to further extract 12 statistical features, viz., Entropy, Homogeneity, Dissimilarity, Energy, Cluster prominence, Cluster shade, Sum of squares, Auto correlation, Maximum probability, Inverse different Moment, Contrast, and Correlation, Then, These features are fed to the SVM to detect exudate and normal region (Ruba&Ramalakshmi 2015).

Xiao et al. have used background estimation method and SVM for classifying exudates. At first, the bright lesions are extracted using background estimation methods. Then, Kirsch operation is used to gather the edge information and remove optical disc and extract the candidate hard exudates region. Then SVM is used to detect the exudate with help of shape feature, phase feature and histogram statistics (Xiao et al. 2015). In Table 1.1, information regarding the results of these methods and the databases used in each study has been summarized.

Table 1.1 State-of-the-art for DR Detection using Exudates Segmentation

Author	Features	Methods	Target Class	Database	Performance
Fleming et al. (2007)	Exudates	SVM	DR, Normal	In house database	Sensitivity= 95% Specificity = 84.6%
Neimeijer et al. (2007)	Exudates	k-NN	DR, Normal	In house data	Sensitivity= 95% Specificity= 86%
Sinthanayothin et al. (2008)	Exudates	Recursive Region Growing Segmentation	DR, Normal	In house data	Sensitivity= 88.5% Specificity= 99.7%
Sopharak et al. (2008)	Exudates	Morphology, Naïve Bayes, SVM	DR, Normal	Hospital database	Sensitivity= 88% Specificity= 99.5%
Sanchez et al. (2008)	Exudates	Thresholding, Fisher	DR, Normal	In house data	Sensitivity= 100% Specificity= 100%
Gracia et al. (2009)	Exudates	MLP, RBF, SVM	DR, Normal	In house data	Sensitivity= 100% Specificity= 92.59%
Jaafar et al. (2010)	Exudates	Thresholding	DR, Normal	DIARETD B	Sensitivity= 91.2% Specificity= 99.3%
Zhang et al. (2014)	Exudates	Morphology	DR, Normal	e-ophtha EX database,	Sensitivity= 96% Specificity= 89%
Xiao et al. (2015)	Exudates	SVM	DR, Normal	DIARETD B, HEMI-MED	Sensitivity=97.3% Specificity=90%

Segmentation of Red Lesions

The red lesions occur in the DR are mainly microaneurysms (MA) and haemorrhages. MAs are tiny lumps in the walls of retinal blood vessels (Fleming et al. 2006; Solomon et al. 2017). In color fundus images, the appearance of MAs is like round red dots, which have a diameter in a range of 10 to 100 µm. It is difficult to distinguish MAs from dot-haemorrhages, as dot-haemorrhages looks similar to MA but slightly larger in size (Tang et al. 2013; Scanlon 2019). MAs are typically the initial symptoms of DR and the quantity of this retinal lesion is directly related to the DR severity (Tang et al. 2013; Solomon et al. 2017). Numerous methodologies have been proposed by various researchers for segmentation of MAs using color fundus image. Table 3.2 shows the various state-of-the-art methods for red lesion detection. Similar to the bright lesion detection methods, the red lesion detection methods can be also distributed into four groups (Mookiah et al. 2013; Salamat, Missen& Rashid 2019).

1. Region Growing Methods

The general concept of region growing method for red lesions detection is similar to that of exudate bright lesion detection. Fleming *et al.*, 2006 have performed region growing on a watershed gradient image to detect candidate red lesion regions. (Jelinek et al. 2006) validated an automatic MA detection method by following the method proposed by (Cree et al. 1997) and (Spencer et al. 1996). The circular, non-connected red lesions are discriminated from blood vessels using a top-hat transformation. Then, candidate lesions are segmented using a region growing algorithm. Li and Chan have proposed a microaneurysm detection method using region growing. In a pre-processed image, all the pixels are considered as non-member of a region. The process initiates from a pixel with the maximum intensity. The algorithm checks the 8-neighboring pixels of the seed pixel and excludes the neighnboring pixel from the region growing if the pixel is already a member. If the neighboring pixel is not already a member then, the absolute difference is computed between the intensity of the neighboring pixel and seed pixel and compred with the pre-defied threshold value. When the difference value exceed the threshold the pixel is not considered as the part of the region in which the seed pixel belongs to. Thus, it remains non-member. When the difference value does not exceed the threshold, the neighboring pixel is considered as the part of the region where the seed point belongs to. Then, the process repeats for each included member pixels until no more pixels left to add. Each clustered region is marked as either microanurysm or non-microaneurysm region based on the ground truth representative points of

microaneurysms. From the candidate regions 12 features are extracted, viz., mean and standard deviation of three color channels, mean and standard deviation of the candidate region, L1 norm, L2 norm, mean absolute deviation, and number of pixels in a region. The extracted 12 features are then fed to artificial neural network (ANN) to classify the microaneurysm and non-microaneurysm region (Li & Shan 2018).

2. Mathematical Morphology Operations

The basic concept of morphological operation has been described in previous section, For red lesion detection, various researchers have used morphological operations. As morphological operation, a polynomial contrast enhancement operation is used to identify MAs in (Walter et al. 2007) and to differentiate between MAs and blood vessels in (Jaafar, Nandi & Al-Nuaimy 2011a). Sreng et al. used top-hat operation to segment the red lesions in DR image. Initially, a pre-processed image is complemented to reverse the intensity values. Then, the background pixels of the images are detected using morphological opening operation. A disc shaped element structure of radius 10 has been used to detect the background. The red lesions are detected by subtracting the background image pixels from the complemented image. The 5 features, viz., perimeter, area, mean of the maximum intensity, minimum intensity and mean intensity of the candidate region are fed into SVM to classify DR and no DR image (Sreng et al. 2018).

3. Wavelet-based Methods

A wavelet-based method is useful when a signal varies over time. It includes various transforms depending on the merit function used for a particular application. Wavelet transform can be discrete or continuous. The discrete wavelet transform decomposes a signal into a set of wavelets of functions orthogonal to the translation and scaling. The generated number of wavelet coefficients is same as that of the data points. Continuous wavelet transform generates a 1D array of vector larger than input data points. A wavelet-based method has been proposed in (Quellec et al. 2008). Using wavelet transform images are discomposed in sub-bands and then based on template matching approach the microaneurysms are identified from the complementary information in each sub-band. Prasad et al. have used wavelet based approach for detection of DR. From a pre-processed image, the histogram equalization and canny edge detection have been used for segmentation of the blood vessels. Then morphological operations are performed to detect microaneurysms and exudates. For feature extraction, area of blood vessels, microaneurysms, and exudates are calculated. Additionally, mean, skewness, entropy, standard deviation, and GLCM are extracted as the features from 4 sub images. The features selection is done by Haar wavelet and Principal Component Analysis (PCA). Haar wavelet discomposes the image into sub-bands and converts 41 features into 65 features. Then, the dimension of the features set is reduced by PCA and a set of 22 features is constructed to feed to a back propagation neural network (BPNN) (Prasad, Vibha & Venugopal 2016).

4. Hybrid Methods

Niemeijer et al. developed a hybrid algorithm for segmentation of red lesions (Niemeijer et al. 2005). The system combined a mathematical morphology based algorithm for candidate selection and a pixel classification algorithm to identify red lesions. Zhang et al. evaluated multi-scale correlation filtering method for candidate detection. The correlation between pixel intensity distributions is calculated for the entire image and a Gaussian model is used for identifying MAs (Zhang et al. 2010). The approach explained by Lazar and Hajdu is based on computing cross-section profiles along multiple directions to generate a multi-directional height map (Lazar & Hajdu 2013).

García *et al.* developed a feature classification method, where a set of features is extracted from the image. The most suitable feature subset is selected, using a feature selection algorithm, for red lesion detection. To obtain the final segmentation result, four Neural Network-based classifiers: radial basis function, support vector machine, multilayer perceptron, and a combination of these three are used through a majority voting scheme (García et al. 2008, 2010). Sánchez *et al.* used a three-class Gaussian mixture-model considering that each pixel in the image belonged to either background or foreground pixels depicting lesions, vessels, or optic disc. The pixels those don't belong to any of these two classes are considered as outliers (Sánchez et al. 2009). Mizutani*et al.* used a modified double ring filter to

extract MAs alongside with blood vessels. In this method, the double ring filter detects the areas of the image having the mean pixel value lower (inner circle) than the mean pixel value in the surrounding area, i.e., outer circle (Mizutani et al. 2009; Inoue et al. 2013). Dashtbozorg et al. have used a hybrid approach for detecting microaneurysm and non-microaneurysm region. By applying gradients weighing technique and iterative thresholding method, various candidate microaneurysm regions are extracted. The candidate features are extracted using local convergence filter (LCF). Along with the LCF features, intensity based features and shape based features are added to construct a feature set. To discriminate microaneurysm and non-microaneurysm region, hybrid boosting/sampling algorithm RUSboost has been used. RUSboost (Seiffert et al. 2010) is a combination of adaptive boosting classifier AdaBoost and random undersampling method (RUS). To particularly work with microaneurysm detection, RUSBoost is coupled with decision tree to detect microaneurysm and non-microaneurysm region (Dashtbozorg et al. 2018).

Table 1.2 State-of-the-art for DR Detection using Red Lesions

Authors	Features	Method	Target Class	Database	Performance
Neimeijer et al. (2005)	Red lesions	Pixel classification using k-NN	DR, Normal	In house database	Sensitivity= 100% Specificity= 87%
Fleming et al. (2006)	Red lesions	Region growing based k-NN	DR, Normal	In house database	Sensitivity= 85.4% Specificity= 83.1%
Jelinek et al. (2006)	Red lesions	Top hat transform and Naïve Bayes	DR, Normal	Hospital database	Sensitivity= 85% Specificity= 90%
Walter et al. (2007)	Red lesions	Gaussian filtering, top-hat transform	DR, Normal	In house database	Sensitivity= 97%
Mizutani et al. (2009)	Red lesions	Double ring filter	DR, Normal	ROC database	Sensitivity= 63.5%
Gracia et al. (2010)	Red lesions	Neural Network	DR, Normal	In house database	Sensitivity= 100% Specificity= 56%
Jaafar et al. (2011)	Red lesions	Morphology based	DR, Normal	DIARETDB	Sensitivity= 98.8% Specificity= 96.2%
Inoue et al. (2013)	Red lesions	Morphology based, PCA, ANN	DR, Normal	ROC database	Sensitivity= 72.9%
Dashtbozorg et al. (2018)	Red lesions	Thresholding, LCF, RUSBoost	DR, Normal	ROC database	Sensitivity score=0.47
				MESSIDOR	AUC= 0.798

Deep Learning Methods

The recent advancement in the deep learning has unlocked the path of a new methodology for retinal image analysis. Especially, Convolutional Neural Network (CNN) has caught the attention of the researchers. Most of these works have used the popular CNN architecture for analyzing the DR images. Gulshan et al. used Inception V3 architecture for detecting moderate and worse diabetic retinopathy, which is considered as referable diabetic retinopathy, then, referable diabetic macular edema, or both. They conducted experiments on EyePACS-1 database consisting of 9963 images and Messidor-2 database consisting of 1748 images. The referable diabetic retinopathy has been defined as when any image fulfilled the criteria 1) moderate, severe or proliferative, (2) referable diabetic macular edema or both. A single network has been trained to make binary predictions about each of these conditions. For detecting referable DR, the algorithm has obtained an area under the receiver operating curve (AUC) of 0.991 for EyePACS-1 and 0.990 for Messidor-2. For EyePACS-1 the sensitivity achieved is 97.5% and specificity is 93.4%. For Messidor-2 database, the sensitivity is 96.1% and specificity is 93.9% (Gulshan et al. 2016).

Doshi et al. has used deep convolutional neural networks for automated diagnosis and classification of five stages of the Diabetic Retinopathy based on severity. They have designed a CNN architecture comprising of five sets of combination of convolution, pooling and dropout layers in sequence. This is tailed by two sets of fully connected hidden and pooling layers. The achieved accuracy of a single trained network is 0.386 on a quadratic weighted kappa metric. The ensemble of three such identical models ensued a kappa score of 0.3996 on the EyePACs dataset database (Doshi et al. 2016).

Haloi et al. has provided a deep learning based automated method for microaneurysm detection. Each pixel of the image is classified as either microaneurysm or non-microaneurysm using a deep neural network with max-out activation function. Their architecture contains five layers including

convolutional, max pooling, Softmax layer, and additional dropout layer. The presented method is evaluated using publicly available Retinopathy Online Challenge (ROC) and Diaretdb1v2 database. For ROC database, the method achieved AUC 0.98. For Diaretdb1v2 database, the methods achieved sensitivity 97%, specificity 95% and AUC 0.98. For DR and no-DR case, the method achieved sensitivity 97%, specificity 96%, and accuracy 96% in Messidor dataset (Haloi 2015).

Chandore et al. has used a deep CNN model of 15 layers to classify DR and non-DR images. Their CNN architecture contains thirteen convolutional layers and two fully connected layers. The layers are arranged as three successive convolution layers tailed by a max-pool layer. A ReLU layer is placed after each convolutional layer and fully connected layer and then, dropout layers are used to deal with overfitting. They experimented on 35,126 labelled high-resolution images from Kaggle dataset. The model has obtained an accuracy of 45% for detecting no DR image and 40% accuracy for detecting DR image. The method has achieved Precision value 0.88 for detecting DR images (ChandoreVishakha 2017).

Lam et al. has carried out experiments on deep learning models for DR grading. They have performed experiments for DR screening using AlexNet, VGG16, and GoogLeNet. These three models are trained and tested on Kaggle and Messidor Mild DR Dataset for binary classification (DR and no-DR). Among all these models GoogLeNet performed the highest. GoogLeNet achieved 95% sensitivity and 96% sensitivity on Kaggle dataset; and obtained 90% sensitivity and 71% specificity for Messidor dataset. For multi-class classification (5 Class) GoogLeNet obtained 75% sensitivity 74% positive predictive value and Kappa value 0.536 (Lam et al. 2018).

Gargeya&Leng have used deep learning for diagnosing DR. Their model attained 0.97 AUC, 94% sensitivity and 98% specificity validated by a 5-fold cross-validation scheme over a local dataset. They also tested the method against MESSIDOR 2 and E-Ophtha databases and attained a 0.94 and 0.95 AUC score, respectively (Gargeya&Leng 2017).

Table 1.3 State-of-the-Art of RVO Detection

Author	Target Class	Method	Remarks
J. Anitha et. al (2009)	CRVO	Fuzzy C-means clustering, Back Propagational Neural Network (BPN)	CRVO is one of the 4 other eye diseases for multiclass classification
Gayathri et al.(2014)	-	Complete Local Binary Pattern, Neural Network	R= 0.98 under Regression plot, R=0.69 for testing.
Zhang et al. (2014)	BRVO	Hierarchical Local Binary Pattern, Support Vector Machine	Accuracy 96.1%.
Zhao et al. (2015)	BRVO	Convolutional Neural Network	Accuracy 97% (images based), 98.5% (patch-based)
Fazekas et. al (2015)	CRVO, BRVO, HRVO	Fractal properties of blood vessels	No performance evaluation
Zode et al (2017)	BRVO	Fractal analysis	No performance evaluation

Discussion on Existing Methodologies for Retinal Blood Vascular Disease Detection
From the literature, the state-of-the-art methods for retinal blood vascular disease detection can be divided mainly into traditional methods and deep learning methods. In the traditional machine learning methods, it can be seen that the majority of the works, either for DR or RVO, practices the hand designed segmentation and feature extraction algorithms for abnormal features such as microaneurysms, haemorrhages, hard exudates, cotton wool spots, and blood vessels to classify the disease. The problem here is that the classification decision relies on the successful segmentation and feature extraction method. On the other hand, the deep learning methods are free from hand designed feature extraction methods. The deep models can extract the features from the image pixels itself. However, these popular deep learning models are highly complex and demand a huge amount of training data, memory, and training time. Tuning the parameters and hyperparameters is still an issue. In the part of DR detection, most of the existing methods show poor performance in detecting DR at the earliest stage as the textural change in the retina during mild NPDR is indistinct.

There are two possible approaches for automatic detection of retinal blood vascular diseases such as DR and RVO. Either follow the traditional method and use hand designed segmentation and feature extraction algorithms to individually extract the abnormal features, then, pass those features through a

classifier to recognize the type of retinal disease (DR or RVO/DR types/RVO types). Otherwise, the abnormal features can be extracted from the appearance of the whole image, and use machine learning classifiers to discriminate between DR and RVO. For detecting all types of RVO compound pattern recognition techniques are required. Again, it is quite challenging to design algorithm in such a way that it can identify the common lesions and distinguish different diseases. Moreover, the performance of the final classification for such conventional CAD methods depends on the quality of the acquired retina image. The factors such as the inter-image and intra-image contrast, color variation, and luminosity make it challenging to identify the abnormal features.

The possible effective way of diagnosing retinal blood vascular disease is the deep learning approach. Because using deep learning it is possible to avoid the burden of complex multifaceted hand-designed feature extraction methods. Therefore, it will significantly reduce the overall complexity of a CAD method and also improve the performance effectively. Only thing should be taken care of is the inherent complexity of the deep learning models and its huge requirement of the resources. It is required to find a way to set the hypothesis for designing simple, effective deep learning models useful for a particular task in hand.

Implementation

Figure 4showsproposed implementation of the retinal vessel segmentation system is enlightenedby transfer learning, which provides theoretical support to apply the fully convolutionalneural network decently in retinal blood vessel segmentation. Themost difficult part in retinal blood vessel segmentation is to distinguish vessels and all theother surrounding tissues / lesions, and the use of efficient semantic segmentation helps toeliminate the noises. There are three innovative points which have eventually made thisproposed work successful. First, the proposed method has shifted, or in another word, simplified the typical retinal vessel segmentation problem from full-size image segmentationto regional vessel element recognition. This is to say, vessel pixels are to be recognized fromregion to region and merged together in the end. Second, because of this problem shifting,the training data, therefore, can be augmented from a hundred to a hundred thousand, which guarantees the effectiveness of deep network training. Third, the proper method of fine tuningthe pre-trained semantic segmentation model has made the regional segmentation task mucheasier.Before processing, the data gathered from the databases will be firstly assigned into the training group and testing group. In both training and the testing phases, both of theoriginaltraining and testing datasets will be pre-processed to enhance the image contrast.Next,every image in each dataset will be split into 50_50 image slice, which is the process of dataaugmentation. The procedure of data augmentation is the essence of this proposed system,not only because it will greatly increase the amount of the dataset, but also because this simplifies the vessel segmentation task from global vascular tree segmentation into regionalvessel portion segmentation. After the preparation of image slices, the training data will beutilized to fine tune the pre-trained fully convolutional Network (AlexNet). Then the testing data willbe fed to the tuned network in order to test the performance of the tuned network. Theresults generated by the network will be collected. In the last stage, the collected result sliceswill be merged into full-size and post-processed with de-noising techniques.
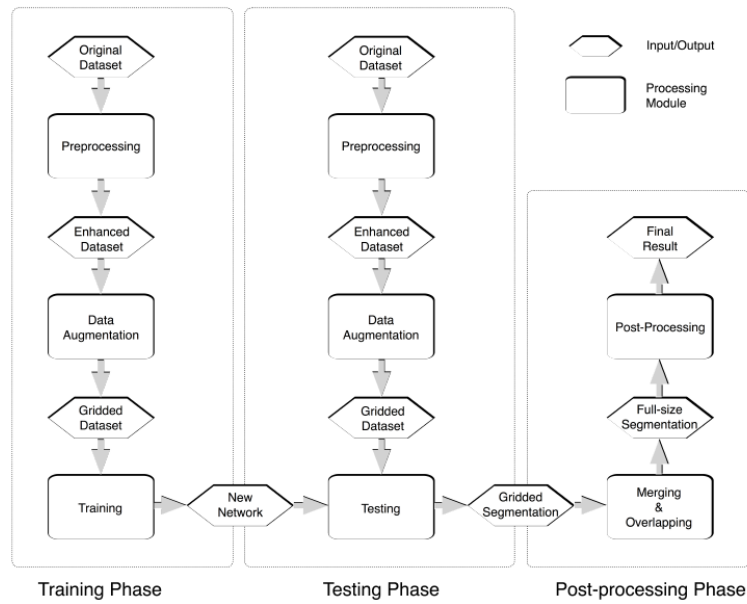
Figure 4: Functional diagram of the supervised retinal vessel segmentation.

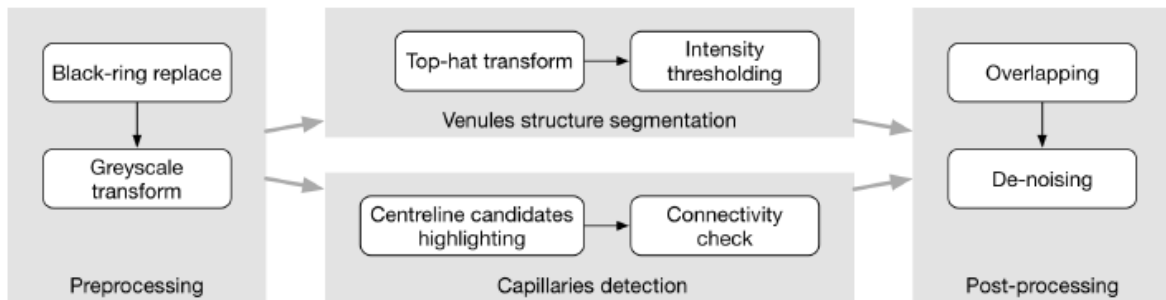The functional block diagram of the proposed system is as shown

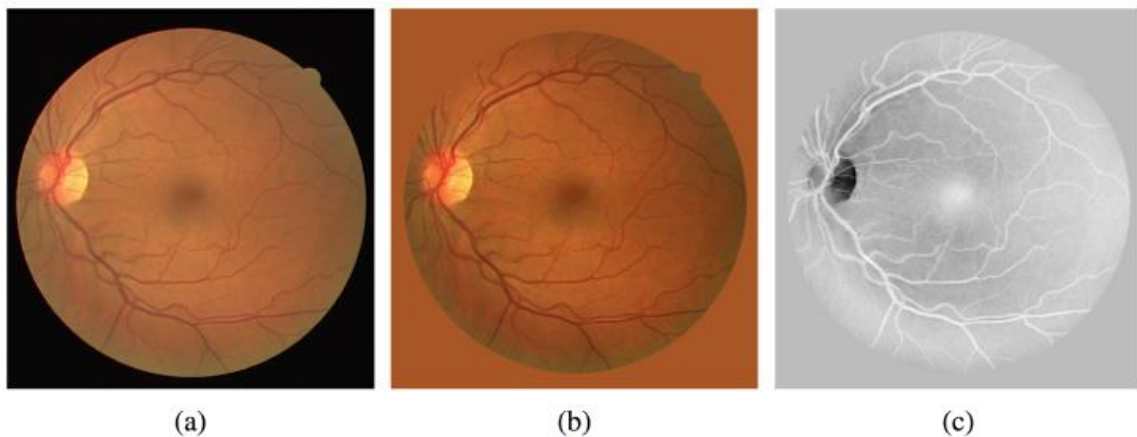Figure 5: Functional diagram of the proposed unsupervised retinal vessel segmentationsystem

Figure 6 Pre-processing phase: (a) original color image, (b) color image after blackring removal, (c) greyscale image after transform through green channel.

Algorithm for CLAHE

Step 1: Divide the original image into non-overlapping sub-regions of size M×N.

Step 2: Calculate the histogram of each sub-region.

Step 3: Histogram of the sub-regions are clipped.

The number of pixels in each sub-region is equally distributed to each gray level. Then, the average

no. of gray value is calculated as $N_{avg} = \frac{NP_{rx} \times NP_{ry}}{N_{gray}}$

Where, N_{avg} = No. of average pixels

NP_{rx} = No. of pixels in x-dimension of the sub-region

NP_{ry} = No. of pixels in y- dimension of the sub-region

N_{gray} = No. of gray levels in the sub-region

$$N_{ACL} = N_{NClip} \times N_{avg}$$

Where, N_{ACL} = Actual clip limit

N_{NC} = Normalized clip limit in the range [0, 1]

The pixels in the original histogram are clipped when the number of pixels is greater than . So, the average pixel distribution in each gray level is computed using the total number of clipped pixels N_{TClip} .

$$N_{AD} = \frac{N_{TClip}}{N_{gray}}$$

Using the above equations, the contrast limited histogram can be calculated using the following clipping rule:

If $H_r(i) > N_{ACL}$, Then $H_{rclip}(i) = N_{ACL}$

Else if $H_r(i) + N_{AD} > N_{ACL}$, Then $H_{rclip}(i) = N_{ACL}$

Else $H_{rclip}(i) = H_r(i) + N_{ACL}$

Where, $H_r(i)$ and H_{rclip} are histograms of the original image and clipped image for each sub-region at i-th level.

Where, $H_r(i)$ and H_{rclip} are histograms of the original image and clipped image for each sub-region at i-th level.

Step 4: After the above distribution, redistribute the remaining clipped pixels N_{RP} and step of the redistributed pixels is given by,

$$S = \frac{N_{gray}}{N_{RP}}$$

The method scans from minimum to maximum gray level to count all the pixels. If the number of pixels is less than N_{ACL}, the program will distribute one pixel to that gray level. If all pixels are not distributed at the end of the search, the new step is calculated using Eq. and start a new search until all the pixels are redistributed.

Step 5: The intensity value in each sub-region is enhanced using histogram equalization. Finally, the pixels in the sub-regions are mapped using bilinear interpolation.
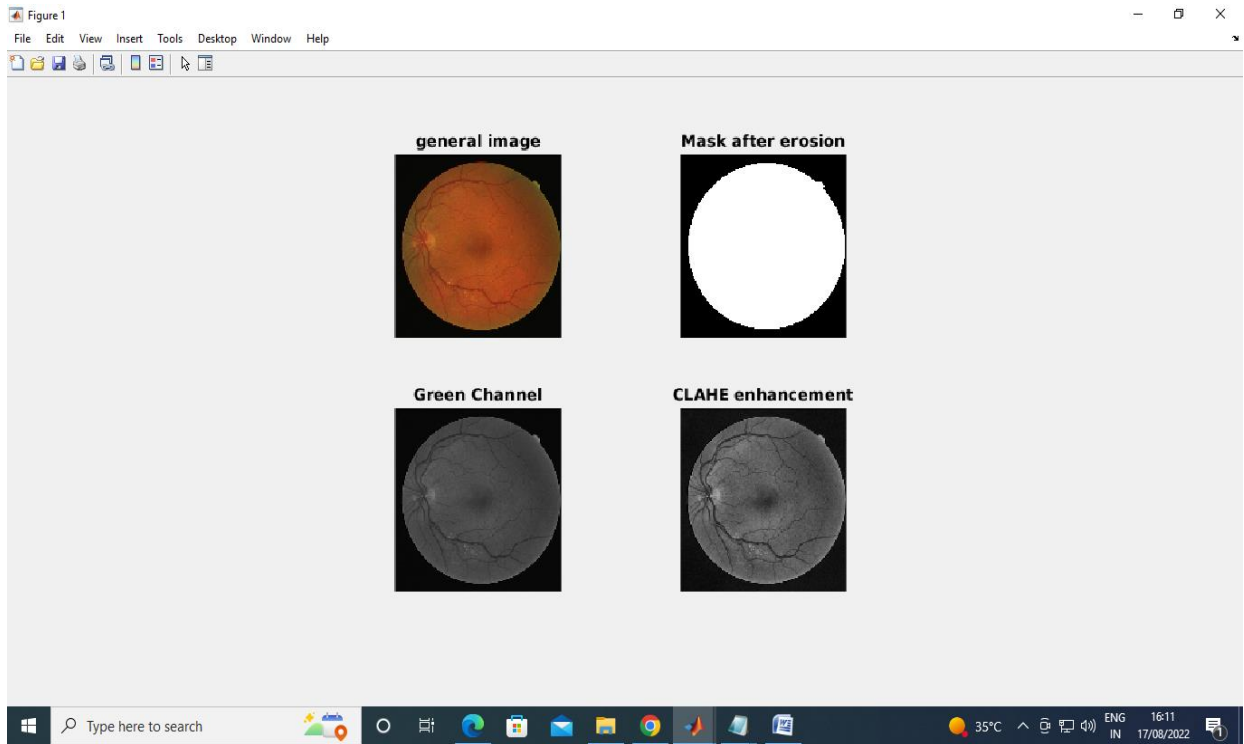
RESULTS

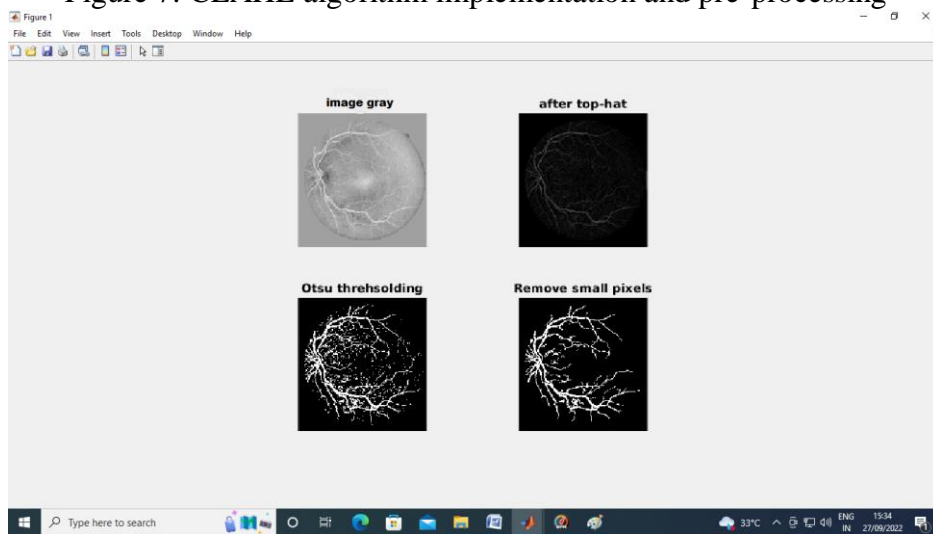Figure 7: CLAHE algorithm implementation and pre-processing

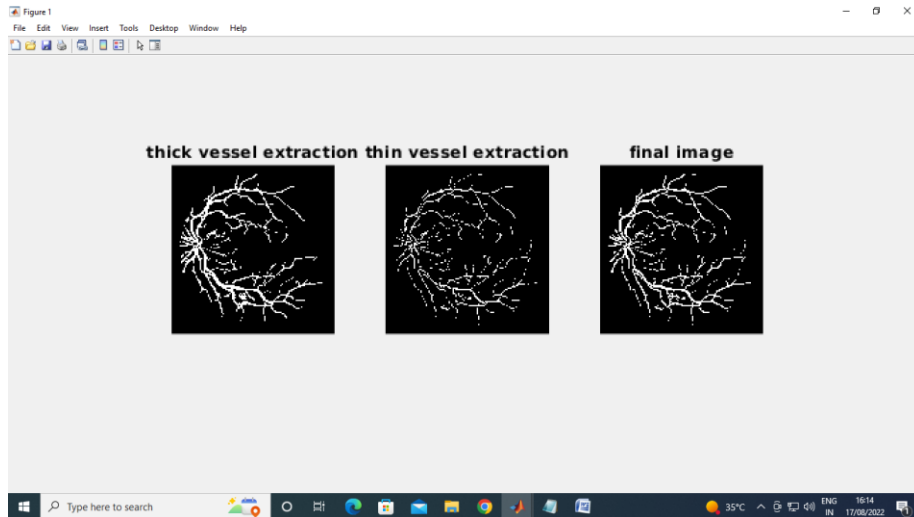Figure 8: OTSU Thresholding and removal of small pixels.

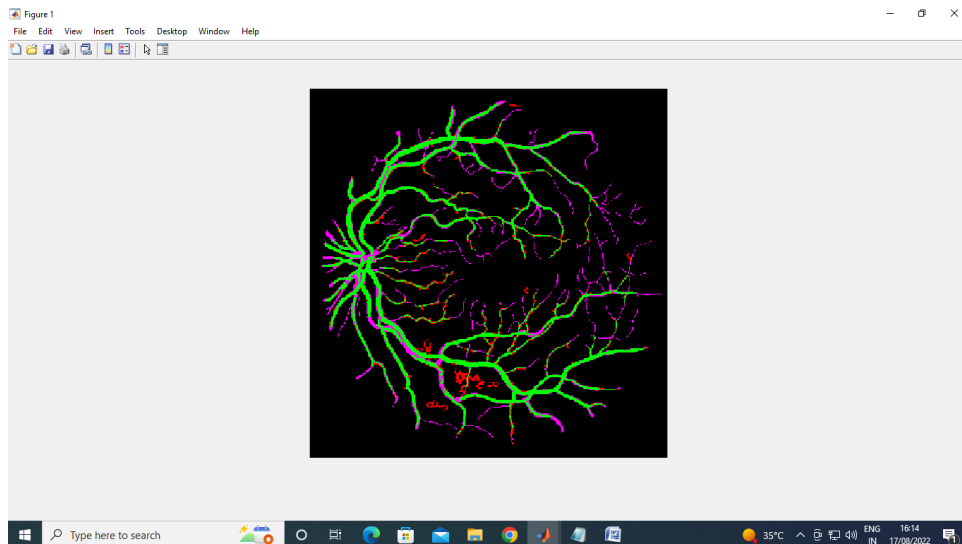Figure 9: Thick, thin vessel extraction and its Final image.

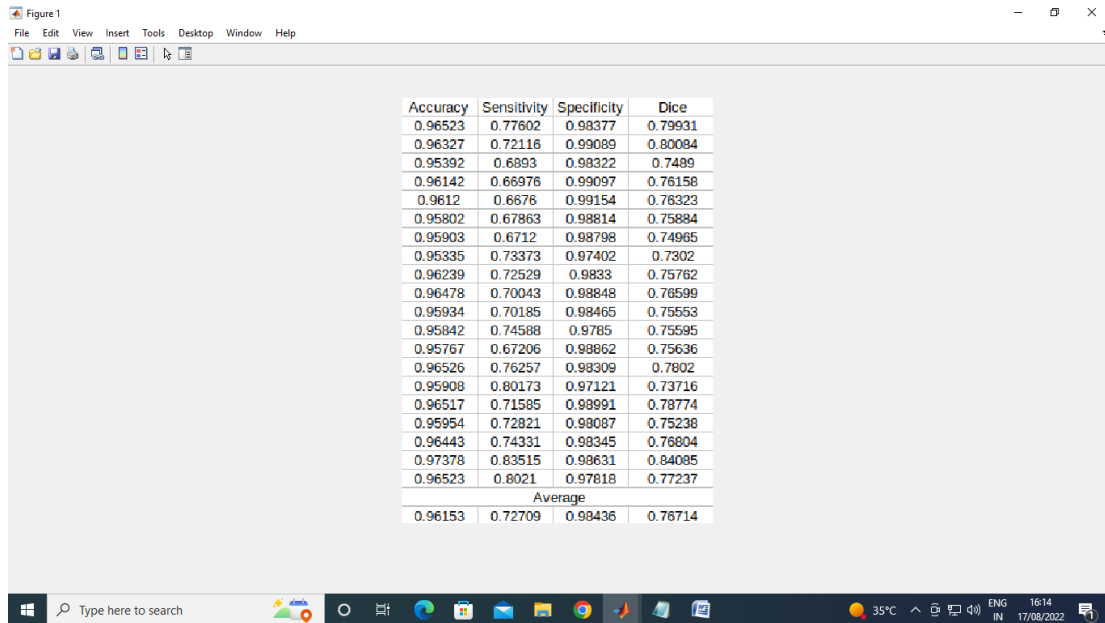Figure 10: Retinal vessels colorized image after process application.

Figure 11: Performance parameters table.

Conclusion

Table 1. Comparison of performance data between different literature methods.

Sl.No	Methods	Accuracy	Sensitivity	Specificity
1	**ZhenweiLi[1]**	**0.9698**	**0.7931**	**0.9896**
2	Wang [2]	0.9511	0.7986	0.9736
3	Chen [3]	0.9453	0.7426	0.9735
4	Strisciuglio [4]	0.9467	0.7731	0.9724
5	Guo [5]	0.9674	0.7891	0.9848
6	Alom [6]	0.9556	0.7792	0.9813
7	**PROPOSED**	**0.97378**	**0.83515**	**0.99089**

The first implementation is a fast, accurate and robust retinal blood vessels segmentationsystem, which uses morphological processing technique to extract vessels and appliesmatched filter algorithm to detect capillaries. These procedures are executed separately butsimultaneously, in order to shorten the execution time while achieving a high accuracy. The second implementation has proposed a supervised method to segment retinal bloodvessel from the retinal color images with the help of the fully convolutional network andtransfer learning. The proposed method has innovatively simplified and shifted a typicalretinal vessel segmentation problem into regional semantic vessel element segmentation tasks,in this way the training data has been ideally augmented. Our proposed method has got improvised values when compared with existing system values. Accuracy, Sensitivity Specificity as mentioned in above table.

References

1. Zhenwei Li *, Mengli Jia, "Blood Vessel Segmentation of Retinal Image Based on Dense-U-Net Network", Micromachines 2021, 12, 1478. https://doi.org/10.3390/ mi12121478.
2. Wang, C.; Zhao, Z.; Ren, Q.; Xu, Y.; Yu, Y. Dense U-net Based on Patch-Based Learning for Retinal Vessel Segmentation. Entropy 2019, 21, 168.
3. Chen, Y. A Labeling-Free Approach to Supervising Deep Neural Networks for Retinal Blood Vessel Segmentation. arXiv2017,arXiv:1704.07502.

4. Strisciuglio, N.; Azzopardi, G.; Vento, M.; Petkov, N. Supervised vessel delineation in retinal fundus images with the automatic selection of B-COSFIRE filters. Mach. Vis. Appl. 2016, 27, 1137–1149.

5. Guo, C.; Szemenyei, M.; Pei, Y.; Yi, Y.; Zhou, W. SD-U-net: A Structured Dropout U-Net for Retinal Vessel Segmentation. In Proceedings of the IEEE 19th International Conference on Bioinformatics and Bioengineering, Athens, Greece, 28–30 October2019; pp. 439–444.

6. Alom, M.Z.; Yakopcic, C.; Hasan, M.; Taha, T.M.; Asari, V.K. Recurrent residual U-Net for medical image segmentation. J. Med.Imaging 2019, 6, 014006.

7. Wang, X.; Jiang, X. Retinal vessel segmentation by a divide-and-conquer funnel-
structured classification framework. SignalProcess. 2019, 165, 104–114.

8. Yan, Z.; Yang, X.; Cheng, K.T. A Three-Stage Deep Learning Model for Accurate
Retinal Vessel Segmentation. IEEE J. Biomed.Health Inform. 2019, 23, 1427–1436.

9. Soomro, T.A.; Afifi, A.J.; Zheng, L.; Soomro, S.; Gao, J.; Hellwich, O.; Paul, M. Deep Learning Models for Retinal Blood Vessels Segmentation: A Review. IEEE Access 2019, 7, 71696–71717.

10. Suryani, E.; Susilo, M. The hybrid method of SOM artificial neural network and median thresholding for segmentation of blood vessels in the retina image fundus. Int. J. Fuzzy Log. Intell. Syst. 2019, 19, 323–331.